IL NUOVO CIMENTO Vol. 34 C, N. 5 Settembre-Ottobre 2011
DOI 10.1393/ncc/i2011-10986-6

Communications: SIF Congress 2010

Measurement of the W-boson production in pp at $\sqrt{s} = 7$ TeV with the ATLAS detector

M. Testa

INFN, Laboratori Nazionali di Frascati - Frascati (RM), Italy

(ricevuto il 28 Dicembre 2010; revisionato il 10 Febbraio 2011; approvato il 10 Febbraio 2011; pubblicato online il 5 Ottobre 2011)

Summary. — In this report I will describe the measurement of the $W \to l\nu$ production cross-section in proton-proton collision at $\sqrt{s} = 7$ TeV with the ATLAS detector. The measurement of the lepton charge asymmetry is also reported. Results are based on data corresponding to an integrated luminosity of approximately $315\,\mathrm{nb}^{-1}$.

PACS 12.15.Lk – Electroweak radiative corrections.
PACS 13.38.-b – Deacys of intermediate bosons.

1. – Introduction

The measurement of the production cross-section of the W-boson constitutes an important test of the Standard Model. Its theoretical prediction depends on the parton distribution functions (PDF) and is affected by significant high-order QCD corrections. The W-boson production cross-section is known at $\sim 4\%$, dominated by PDF uncertainties. Therefore its measurement allows precise tests of QCD to be performed. In addition, the measurement of the charge asymmetry in the $W \to l\nu$ decay as a function of the pseudorapidity of the lepton will constrain the PDFs in an unexplored kinematic region of low parton momentum fraction at large scales. Finally, the production of the W-boson is an important background for several physics searches.

The study of the $W \to l\nu$ channel is also important for commissioning and performance issues. It provides a large sample of isolated high-p_T leptons, and therefore allows the calibration of energy and momentum scale and the study of missing-transverse-energy (E_T^{miss}) performance.

2. – The ATLAS detector and data sample

The ATLAS detector [1] comprises an inner detector (ID) system surrounded by a thin superconducting solenoid, a calorimeter system and three large instrumented superconducting coils, forming the muon spectrometer. Data used for this measurement

were collected from March to July 2010 corresponding to about $315\,\mathrm{nb}^{-1}$ of integrated luminosity. The uncertainty on the absolute luminosity determination is 11% [2]. Events are selected using only the hardware based level 1 (L1) trigger, based on measurements in the calorimeters, in the resistive plate chambers (RPC) and in the thin gap chambers (TCG) of the muon spectrometer, as explained in the next sections.

3. – Electrons reconstruction

Electrons are selected using the L1 calorimeter trigger. It requires coarse-granularity clusters with $|\eta| < 2.5$ and transverse energy $E_T > 10\,\mathrm{GeV}$. The offline reconstruction [3] uses clusters with $E_T > 10\,\mathrm{GeV}$, matched to ID tracks. It provides three quality levels of identification with different efficiency and rejection power:

- *Loose*: the selection uses shape information from the 2nd sampling of the electromagnetic calorimeter and leakage in the hadronic calorimeter
- *Medium*: additional shape information from the 1st sampling, track quality variables and cluster-track matching variables are also used
- *Tight*: the selection exploits also high threshold hits from the transition radiation tracker, conversion rejection and matching of the cluster energy with the momentum of the associated track.

The corresponding efficiencies for the medium and tight selection are 94.3% and 74.9%, relative to the basic reconstruction efficiency of 97%. They are obtained using $Z \to ee$ and $W \to e\nu$ Monte Carlo samples. Corresponding rejection powers against hadrons and electrons from conversions are 5700 and 77000, obtained using QCD dijet background Monte Carlo samples.

4. – Muons reconstruction

Muons are selected using the L1 muon trigger which requires a 3D coincidence of hits in the RPC or in the TCG, along a road which is consistent with the path of high-p_T muons coming from the origin. The width of the road is related to the p_T threshold, which for this analysis is 6 GeV.

The offline reconstruction [4] makes use of combined tracks, *i.e.* associates tracks measured from the muon spectrometer to that measured from the ID. The combined-track parameters are derived from a statistical combination of the two tracks. The muon reconstruction efficiency is 93% as obtained from data. It is calculated by requiring one combined muon to come from the $Z \to \mu\mu$ decay and the other to be an ID track with opposite charge and forming with the former muon an invariant mass consistent with the Z-boson mass.

5. – Missing-transverse-energy reconstruction

The transverse missing energy (E_T^{miss}) is reconstructed from calibrated 3D topological clusters [5]. The calibration takes into account the different response to hadrons than to electrons and photons, dead material and out-of-cluster energy losses [6]. For the electron channel, the components of E_T^{miss} are calculated by summing over all topological clusters energies $E_{x,y}^{miss}|_e = -\sum E_{x,y}^i$. The E_T^{miss} in the muon channel is calculated by adding also the reconstructed momenta of muons: $E_{x,y}^{miss}|_\mu = -\sum E_{x,y}^i - \sum_\mu p_{x,y}^\mu$.

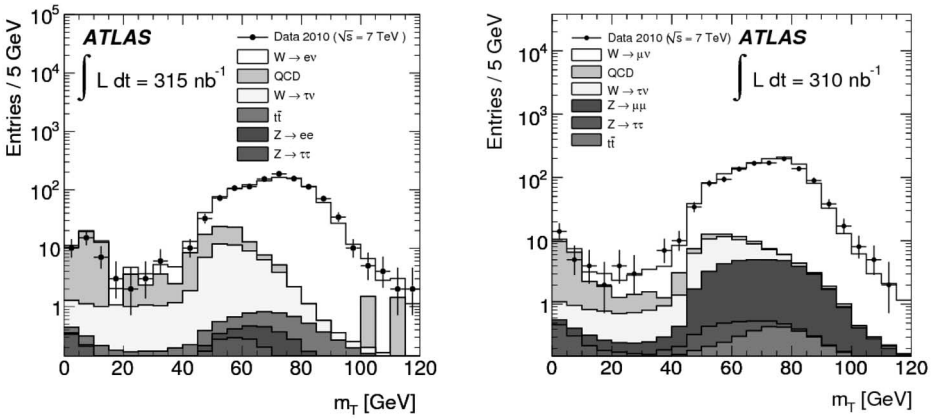

Fig. 1. – Transverse-mass distribution of the electron-E_T^{miss} system (left) and muon-E_T^{miss} system (right) for data and Monte Carlo simulation, broken down into the signal and background components.

6. – Selection of $W \to l\nu$ candidates

Collision candidates are selected by requiring a primary vertex with at least three tracks, consistent with the beam-spot position. Electrons are selected using the "tight" level of identification and are required to have a cluster of $E_T > 20\,\text{GeV}$ within $|\eta| < 2.47$ excluding the transition region between the barrel and the endcap calorimeters ($1.37 < |\eta| < 1.52$).

Muon candidates are required to be combined muons (sect. **4**) with $p_T > 20\,\text{GeV}$, and to have a muon-spectrometer track with $p_T > 10\,\text{GeV}$ within the range $|\eta| < 2.4$. A better signal-to-background ratio is obtained by requiring $\sum p_T^{ID}/p_T < 0.2$, where the sum runs over the transverse momenta of the tracks in the ID within a cone of $\Delta R < 0.4$ around the muon track. This cut rejects 84% of the expected QCD background, while retaining 98% of the signal.

Additional kinematic cuts are then applied: the E_T^{miss} is required to be larger than 25 GeV, the transverse mass of the lepton-neutrino system, m_T should be larger than 40 GeV, where $m_T = \sqrt{2p_T E_T^{miss}(1-\cos\Delta\phi)}$ and ϕ is the azimuthal separation between the directions of the lepton and the E_T^{miss} vector. In fig. 1 the transverse mass distributions for the electron and muon system for events with $E_T^{miss} > 25\,\text{GeV}$ are shown. After the selection, a total of 1069 (1181) candidates are selected for the electron (muon) channel. A complete description of the analysis can be found in [7].

7. – Background estimate

Background contamination due to electroweak (EW) process and to $t\bar{t}$ processes are evaluated from Monte Carlo simulation. QCD background processes are determined from data, owing to the large uncertainty in the predictions of their cross-section production. In the electron channel, QCD background is estimated using the E_T^{miss} distribution. Events were selected applying all the cuts described above, except that on E_T^{miss}. Signal and background yields are obtained from a binned maximum-likelihood template fit. The shapes of the signal, and the dominant $W \to \tau\nu$ EW background process are taken from Monte Carlo simulation, while the shape of QCD processes is derived from data. This QCD template is obtained reversing some of the requirements in the "tight" electron

TABLE I. – *Numbers of observed candidate events for the signal, electroweak plus $t\bar{t}$ and QCD background processes.*

l	Observed candidates	Background (EW+$t\bar{t}$)	QCD background	Background subtracted signal
e	1069	$33.5 \pm 0.2 \pm 3.0$	$28.0 \pm 3.0 \pm 10.0$	$1007.5 \pm 32.7 \pm 10.8$
μ	1181	$77.6 \pm 0.3 \pm 5.4$	$22.8 \pm 4.6 \pm 8.7$	$1080.6 \pm 34.4 \pm 11.2$

identification and rejecting isolated candidates. In the signal region ($E_T^{miss} > 25\,\text{GeV}$) the number of QCD background events is found to be $N_{QCD} = 28.0 \pm 3.0_{stat} \pm 10.0_{syst}$, where the statistical error is due to the statistics of data and templates. The systematic uncertainty is obtained varying the shape of the background template by applying different selection cuts. For the muon channel the contributions from $Z \to \mu\mu$, $W \to \tau\nu$ and $Z \to \tau\tau$ EW processes are expected to be 38.4, 33.6, 1.4 events, respectively, while the $t\bar{t}$ contribution is expected to be 4.2 events. The QCD background is dominated by heavy-quark decays, with smaller contribution from pion and kaon decays and hadrons faking muons. Owing to the large uncertainty in the dijet cross-section and the difficulty on simulating fake prompt muons, the QCD background (N_{QCD}) is derived from data. It is obtained by considering the number of events after the full selection (N_{iso}) and that observed if the muon isolation is not required (N_{loose}) and solving the equations: $N_{loose} = N_{nonQCD} + N_{QCD}$ and $N_{iso} = \epsilon^{iso}_{nonQCD} N_{nonQCD} + \epsilon^{iso}_{QCD} N_{QCD}$, where N_{nonQCD} includes the signal and the non-QCD background processes, and ϵ^{iso}_{nonQCD} and ϵ^{iso}_{QCD} are the efficiencies of the muon isolation requirements for the two event classes. ϵ^{iso}_{nonQCD} is obtained from data using a $Z \to \mu\mu$ sample, while ϵ^{iso}_{QCD} is obtained from a data sample with muons of p_T in the range 15–20 GeV, which is dominated by dijet events. The efficiencies are then extrapolated to higher p_T using Monte Carlo simulation. Using this method the QCD background contribution is estimated to be $21.1 \pm 4.5_{stat} \pm 8.7_{syst}$ events. The systematic uncertainty is dominated by the uncertainty on ϵ^{iso}_{QCD}.

Background contamination from cosmic rays is estimated to be 1.7 ± 0.8 events and is obtained looking at cosmic-ray muons from non-collision bunches that pass the full W-boson selection but fail the primary vertex selection.

The number of observed candidates, the estimated background events from electroweak, $t\bar{t}$ and QCD processes are summarized in table I. The systematic uncertainty includes experimental uncertainty, theoretical uncertainty on the predicted cross-section for W, Z and $t\bar{t}$ production and uncertainties on the PDFs. The luminosity uncertainty of 11% enters in the estimation of the electroweak and $t\bar{t}$ background contributions as they are determined from Monte Carlo simulation.

8. – Cross-section measurement

The production cross-section for the W-boson times the branching ratio for decays into leptons can be expressed as: $\sigma \cdot \text{BR}(W \to l\nu) = \frac{N^{sig}}{A \cdot C \cdot L}$, where N^{sig} is the number of signal events after background subtraction, A is the acceptance for W decays, defined as the fraction of events passing the geometrical and kinematical cuts at the generator level, C is the ratio between the number of events passing the selection cuts and the number of events within the acceptance. This correction factor includes trigger, reconstruction and identification for W-bosons efficiencies. L is the integrated luminosity.

TABLE II. – *Summary of contributions to the uncertainty on C for the electron channel.*

Parameter	$\delta C/C(\%)$
Trigger efficiency	< 0.2
Material effect, reconstruction and identification	5.6
Energy scale and resolution	3.3
E_T^{miss} scale and resolution	2.0
Problematic regions in the calorimeter	1.4
Pile-up	0.5
Charge misidentification	0.5
Final-state radiation modeling	0.3
PDFs	0.3
Total uncertainty	7.0

The C correction factor can be factorized as: $C = \epsilon_{event} \cdot \alpha_{reco} \cdot \epsilon_{lep} \cdot \epsilon_{trig}$, where ϵ_{event} accounts for event selection efficiency (primary vertex), ϵ_{lep} for lepton reconstruction and identification efficiency and ϵ_{trig} for trigger efficiency. α_{reco} accounts for differences observed when applying cuts at the generator or at the reconstruction level. The individual factors are computed from Monte Carlo simulation, except for the trigger efficiency correction for muons which is obtained from data. The central value and the relative uncertainty of C are 0.659 (0.758) and 7.0% (4.0%) for the electron (muon) channel. The contributions on the uncertainty are shown in tables II and III. For the electron channel, the uncertainty is dominated by uncertainties on the electron reconstruction efficiency, by material effects in the ID and by uncertainties in the electron energy scale and resolution. For the muon channel, the total uncertainty is dominated by that on the reconstruction efficiency and on the E_T^{miss} scale and resolution.

9. – Acceptance determination

The acceptance is calculated as the fraction of events passing the kinematical and geometrical cuts applied in the analysis. It is calculated using the PYTHIA Monte Carlo

TABLE III. – *Summary of contributions to the uncertainty on C for the muon channel.*

Parameter	$\delta C/C(\%)$
Trigger efficiency	1.9
Reconstruction efficiency	2.5
Momentum scale	1.2
Momentum resolution	0.2
E_T^{miss} scale and resolution	2.0
Isolation efficiency	1.0
PDFs	0.3
Total uncertainty	4.0

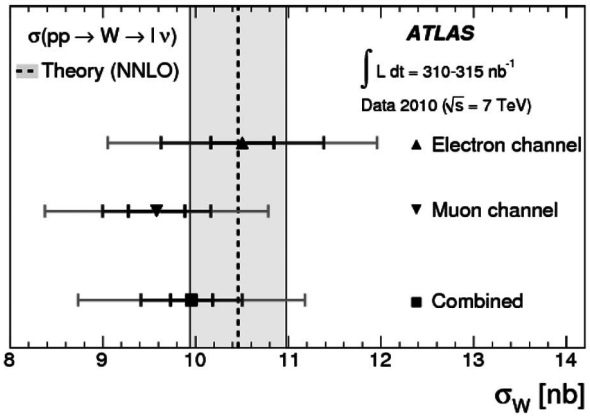

Fig. 2. – Measured value of $\sigma_W \cdot \mathrm{BR}(W \to l\nu)$ compared to the theoretical predictions based on NNLO calculations. The error bands represent successively statistical, statistical plus systematic, and total uncertainties (including the luminosity uncertainty).

generator using the modified leading order PDF set MRST LO* [8]. The central value is 0.465 (0.480) for the electron (muon) channel. The uncertainty is dominated by the limited knowledge on the PDFs and on the modeling of the W-boson production at LHC. The uncertainty is obtained from three contributions. The first is given by the uncertainty within one set of PDFs using CTEQ 6.6 PDFs [9] and is found to be 1.0% and 1.8% for W^+ and W^-, respectively. The second and largest contribution is obtained by using different PDFs sets, MRST LO*, CTEQ 6.6 and HERAPDF 1.0 [10], giving relative uncertainties of 2.7% and 0.9% for W^+ and W^-, respectively. The third contribution due to the production modeling is obtained by comparing results with different generators, Pythia and MC@NLO and the same PDF set (CTEQ 6.6). The resulting relative uncertainty is 0.4% and 1.4% for W^+ and W^-, respectively. A total uncertainty of 3% on the acceptance for W decays is considered in this analysis.

10. – Results and comparison to theoretical expectations

The results for the W-boson production cross-section times the leptonic branching ratios are: $\sigma_{W^+} \cdot \mathrm{BR}(W \to l\nu) = 5.93 \pm 0.17(\mathrm{stat}) \pm 0.30(\mathrm{syst}) \pm 0.65(\mathrm{lumi})\,\mathrm{nb}$, $\sigma_{W^-} \cdot \mathrm{BR}(W \to l\nu) = 4.00 \pm 0.15(\mathrm{stat}) \pm 0.20(\mathrm{syst}) \pm 0.44(\mathrm{lumi})\,\mathrm{nb}$, $\sigma_W \cdot \mathrm{BR}(W \to l\nu) = 9.96 \pm 0.23(\mathrm{stat}) \pm 0.50(\mathrm{syst}) \pm 1.10(\mathrm{lumi})\,\mathrm{nb}$, where lepton universality is assumed.

The theoretical prediction on the W-boson production cross-section times the leptonic branching ratios includes next-to-next-to-leading–order QCD corrections and is based on calculations using the FEWZ [11] and ZWPROD [12, 13] programs with the MSTW 08 NNLO structure function parametrization [14]. They are $\sigma^{NNLO}_{W^+ \to l^+\nu} = 6.16 \pm 0.31\,\mathrm{nb}$, $\sigma^{NNLO}_{W^- \to l^-\nu} = 4.30 \pm 0.21\,\mathrm{nb}$, $\sigma^{NNLO}_{W \to l\nu} = 10.46 \pm 0.52\,\mathrm{nb}$. An overall uncertainty of 5% was estimated using the MSTW 08 NNLO PDF error eigenvectors at 90% CL limit. The comparison to the experimental result is shown in fig. 2.

In fig. 3 the results are compared to previous measurements of the W-boson production cross-section performed by the UA1 [15] and UA2 [16] experiments at $\sqrt{s} = 0.63\,\mathrm{TeV}$ at the CERN $Sp\bar{p}S$, by the CDF [17] and D0 [18] experiments at $\sqrt{s} = 1.8\,\mathrm{TeV}$ and $\sqrt{s} = 1.96\,\mathrm{TeV}$ and by the recent measurement by the PHENIX experiment [19] at

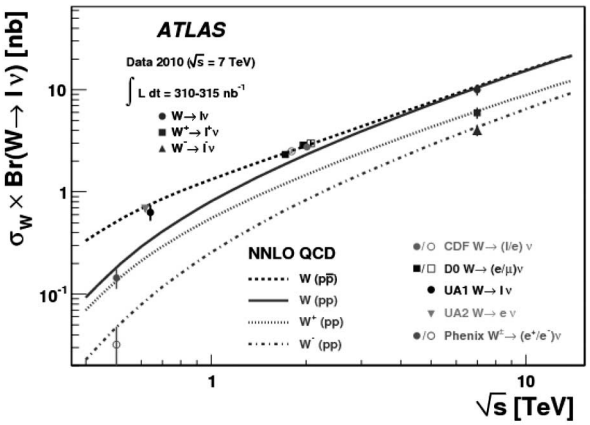

Fig. 3. – Measured value of $\sigma_W \cdot \mathrm{BR}(W \to l\nu)$ for W^+, W^- and their sum compared to theoretical expectations as a function of $\sqrt{s}$. Previous measurements at proton-antiproton and proton-proton collisions are also shown.

$\sqrt{s} = 0.5\,\mathrm{TeV}$. The theoretical predictions of the W-boson production cross-sections are in good agreement with all measurements and their energy dependence is well reproduced as well.

11. – Charge asymmetry

The measurement of the W-boson charge asymmetry is obtained from the charge of the decay leptons and is defined as $A_l = \frac{\sigma^{fid}_{W^+} - \sigma^{fid}_{W^-}}{\sigma^{fid}_{W^+} + \sigma^{fid}_{W^-}}$, where σ^{fid}_W, is the cross-section defined in sect. **8**, without dividing for the acceptance. The overall asymmetry is different from zero, due to the different content of the u and d valence quarks in the proton. Moreover its dependence on the lepton pseudo-rapidity provides constraints on the PDFs, since different pseudo-rapidity regions probe different values of the momentum

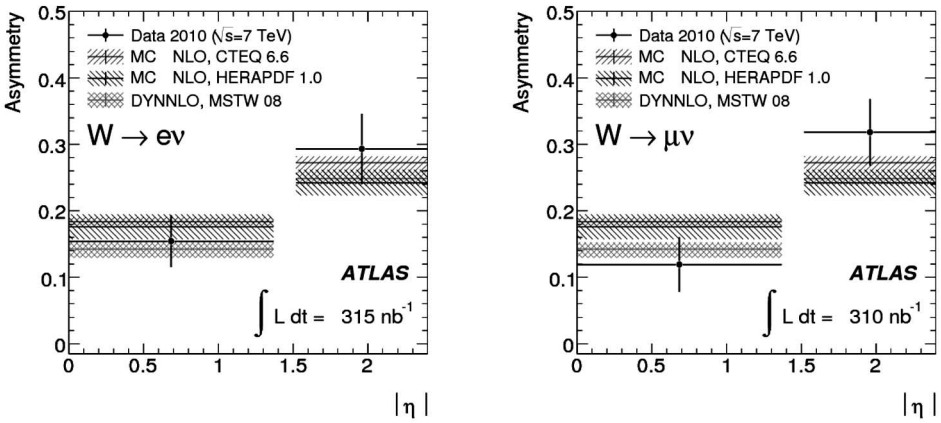

Fig. 4. – Lepton charge asymmetry for the electron (left) and muon (right) channel. The bands represent the uncertainties of several theoretical predictions, obtained from variation of error eigenvector sets of PDFs at the 90% CL.

fraction of the parton producing the W-boson. The asymmetry is measured in two bins of pseudo-rapidity. The precision is limited by the statistical uncertainty. For the electron channel, the major contributions to the systematic uncertainty are the uncertainties on the electron identification, on the charge misidentification, on the energy scale and on the background subtraction. For the muon channel, the systematic uncertainty is dominated by the uncertainty on the muon momentum scale and resolution, on the trigger efficiency and on the background subtraction. The measured lepton asymmetry is shown in fig. 4 and compared to the theoretical predictions obtained with NLO calculations, MC@NLO [20] and DYNNLO [21], interfaced with various PDFs of the corresponding order. Within the large uncertainties, the theoretical predictions agree with the measurements. However, data do not yet provide sufficient separation between the different models.

REFERENCES

[1] The ATLAS Collaboration, *JINST*, **3** (2008) S08003.
[2] The ATLAS Collaboration, *Luminosity determination using the ATLAS detector* ATLAS conference note: ATLAS-CONF-2010-060, `http://cdsweb.cern.ch/record/1281333`.
[3] The ATLAS Collaboration, *Electron and photon reconstruction and identification in ATLAS: expected performance at high energy and results at* $\sqrt{s} = 900\,GeV$, ATLAS conference note: ATLAS-CONF-2010-005, `http://cdsweb.cern.ch/record/1273197`.
[4] The ATLAS Collaboration, *Expected performance of the ATLAS experiment: detector, trigger and physics*, CERN-OPEN-2008-020, arXiv:0901.0512[hep-ex].
[5] Lampl W. *et al.*, *Calorimeter clustering algorithms: description and performance*, ATLAS note: ATLAS-LARG-PUB-2008-002, `http://cdsweb.cern.ch/record/1009735`.
[6] Barillari T. *et al.*, *Local calibration*, ATLAS note: ATLAS-LARG-PUB-2009-001, `http://cdsweb.cern.ch/record/11112035`.
[7] Measurement of the $W \to l\nu$ and $Z/\gamma^* \to ll$ production cross-sections in proton-proton collisions at $\sqrt{s} = 7\,\text{TeV}$ with the ATLAS detector, CERN-PH-EP-2010-037, arXiv:1010.2130[hep-ex].
[8] Sherstenv A. and Thorne R. S., *Eur. Phys. J. C*, **55** (2008) 553.
[9] Nadolsky P. M. *et al.*, *Phys. Rev. D*, **78** (2008) 97.
[10] Aaron F. D. *et al.* (The H1 and ZEUS Collaboration), *JHEP*, **01** (2010) 109.
[11] Anastasion C., Dixon L. J., Melnikov K. and Petriello F., *Phys. Rev. D*, **69** (2004) 094008.
[12] Hamberg R., van Neerven W. L. and Matsuura T., *Nucl. Phys. B*, **359** (1991) 343; **644** (2002) 403 (Erratum).
[13] van Neerven W. L. and Zijlstra E. B., *Nucl. Phys. B*, **382** (1992) 11, **680** (2004) 513 (Erratum).
[14] Martin A. D., Stirling W. J., Thorne R. S. and Watt G., *Eur. Phys. J. C*, **63** (2009) 189.
[15] Albajar C. *et al.* (The UA1 Collaboration), *Phys. Lett. B*, **198** (1987) 271.
[16] Alitti J. *et al.* (The UA2 Collaboration), *Phys. Lett. B*, **276** (1992) 365.
[17] Abulencia A. *et al.* (The CDF Collaboration), *J. Phys. G*, **34** (2007) 2457.
[18] The D0 Collaboration, D0 conference notes: 4403-CONF, 4570-CONF.
[19] Adare A. *et al.* (PHENIX Collaboration), *Cross Section and Parity Violating Spin Asymmetry of* $W^{/pm}$ *Boson Production in Polarized p+p Collisions at* $\sqrt{s} = 500\,GeV$, arXiv:1009.0505 [hep-ex].
[20] Catani S. and Grazzini M., *Phys. Rev. Lett.*, **98** (2007) 222002.
[21] Frixione S. and Webber B. R., *JHEP*, **0206** (2002) 29.